SIGNIFICANCE OF IMPROVED FOURIER-FICK LAWS IN NON-LINEAR CONVECTIVE MICROPOLAR MATERIAL STRATIFIED FLOW WITH VARIABLE PROPERTIES

by

Muhammad WAQAS[a*], Muhammad Ijaz KHAN[a], Shahid FAROOQ[a], Tasawar HAYAT[a,b], and Ahmed Al-SAEDI[b]

[a] Department of Mathematics, Quaid-i-Azam University, Islamabad, Pakistan
[b] Nonlinear Analysis and Applied Mathematics (NAAM) Research Group, Department of Mathematics, Faculty of Science, King Abdulaziz University, Jeddah, Saudi Arabia

Original scientific paper
https://doi.org/10.2298/TSCI171027285W

Present research article describes the effectiveness of improved Fourier-Fick fluxes and temperature-dependent conductivity on the 2-D, incompressible steady micropolar material flow over a stretchable surface. Non-linear mixed convection, double stratification and heat generation aspects are considered. The considered flow non-linear PDE are converted to ODE via appropriate transformations. Through implementation of homotopy method the obtain system is solved for series solutions. The effects of pertinent parameters are discussed through graphical sketch. Skin friction coefficient (drag force) is calculated. Main findings are pointed out.

Key words: *improved Fourier-Fick fluxes, micropolar material flow, improved Fourier's expression, double stratification, temperature-dependent conductivity, stagnation point flow*

Introduction

To elaborate the energy transportation through heat conduction, the well-known Fourier relation has been extensively applied in engineering utilizations [1]. Heat conduction expression via Fourier situation has parabolic nature which permits thermal instabilities to communicate thermal propagation of wave having infinite speed and requires to be improved at extremely smaller time scales and length in a few nano or micro-scale structures [2]. A well-known methodology in which limited velocity of thermal wave proliferation is accounted via relaxation time concept is initiated which turns heat conduction expression from parabolic form to the hyperbolic one [3-5]. Numerous researchers have contributed further developments subjected to Cattaneo model [3]. Christov [6] modified Cattaneo model [3] via insertion of upper-convected Oldroyd's derivative. Some researches elaborating flow subjected to Cattaneo-Christov (non-Fourier) heat flux are given in [7-12].

Among numerous models of non-Newtonian materials, the micropolar material model has acquired ample consideration in view of the fact that it is capable to illustrate the micro-motions and local structure features of liquid components which are overlooked by traditional models. Several real materials (liquid crystals, animal blood, polymeric suspensions, muddy fluids, small scales water models *etc.*) reveal microscopical characteristics (like rotation) being

* Corresponding author, e-mail: mwaqas@math.qau.edu.pk

effectively described through micropolar material model. From physical viewpoint, this model elaborates materials involving large quantity of tiny spherical components uniformly disseminated inside the viscous medium. Related rheological model is established on novel vector field introduction and rotating particles (microrotation) angular velocity field. Accordingly, one novel vector expression is inserted to Navier-Stokes structure coming from angular momentum conservation. Therefore, we finish off with a multifaceted (coupled) PDE system fulfilled by velocity of fluid, microrotation and pressure with four novel viscosities established. The micropolar material model was initially modeled by Eringen [13]. Lukaszewicz [14] presents a monograph which comprehensively addresses the novel mathematical concept covering this unique model. Afterwards numerous investigators consider micropolar material subjected to distinct aspects (see [14-18]).

Here micropolar material flow near a stagnant point is formulated in frames of modified Fourier-Fick laws and heat generation. Variable fluid properties (temperature-dependent conductivity) and double stratification characteristics are considered. Homotopy solutions [19-25] are established for developed systems. Physical interpretation is given for various aspects of sundry variables against the profiles of velocity, thermal and solutal fields.

Formulation

Here incompressible micropolar material stagnation point flow highlighting the non-Fourier-Fick fluxes is modeled. The concept of heat generation is utilized for energy expression formulation. Double stratification and variable fluid properties (temperature-dependent conductivity) are also considered. Non-linear version of mixed convection is introduced. Application of boundary-layer theory yields the following governing expressions [15]:

$$\frac{\partial u}{\partial x}+\frac{\partial v}{\partial y}=0 \tag{1}$$

$$u\frac{\partial u}{\partial x}+v\frac{\partial u}{\partial y}=\left(\nu+\frac{k}{\rho}\right)\frac{\partial^2 u}{\partial y^2}+\frac{k}{\rho}\frac{\partial N}{\partial y}+g\begin{pmatrix}\beta_1(T-T_\infty)+\beta_2(T-T_\infty)^2+\\+\beta_3(C-C_\infty)+\beta_2(C-C_\infty)^2\end{pmatrix}+U_e(x)\frac{\mathrm{d}U_e(x)}{\mathrm{d}x} \tag{2}$$

$$u\frac{\partial N}{\partial x}+v\frac{\partial N}{\partial y}=\frac{\gamma^*}{\rho j}\frac{\partial^2 N}{\partial y^2}-\frac{k}{\rho j}\left(2N+\frac{\partial u}{\partial y}\right) \tag{3}$$

$$u\frac{\partial T}{\partial x}+v\frac{\partial T}{\partial y}+\lambda_1\begin{pmatrix}u\dfrac{\partial u}{\partial x}\dfrac{\partial T}{\partial x}+v\dfrac{\partial v}{\partial y}\dfrac{\partial T}{\partial y}+v\dfrac{\partial u}{\partial y}\dfrac{\partial T}{\partial x}+\\+2uv\dfrac{\partial^2 T}{\partial x\partial y}+u^2\dfrac{\partial^2 T}{\partial x^2}+v^2\dfrac{\partial^2 T}{\partial y^2}-\\-\dfrac{Q}{\rho c_p}\left(u\dfrac{\partial T}{\partial x}+v\dfrac{\partial T}{\partial y}\right)\end{pmatrix}=\frac{1}{\rho c_p}\frac{\partial}{\partial y}\left[K(T)\frac{\partial T}{\partial y}\right]+\frac{Q}{\rho c_p}(T-T_\infty) \tag{4}$$

$$u\frac{\partial C}{\partial x}+v\frac{\partial C}{\partial y}+\lambda_2\begin{pmatrix}u\dfrac{\partial u}{\partial x}\dfrac{\partial C}{\partial x}+v\dfrac{\partial v}{\partial y}\dfrac{\partial C}{\partial y}+v\dfrac{\partial u}{\partial y}\dfrac{\partial C}{\partial x}+\\+2uv\dfrac{\partial^2 C}{\partial x\partial y}+u^2\dfrac{\partial^2 C}{\partial x^2}+v^2\dfrac{\partial^2 C}{\partial y^2}\end{pmatrix}=D\frac{\partial^2 C}{\partial y^2}, \tag{5}$$

$$u = U_w(x) = cx,\ v = 0,\ N = -m_0 \frac{\partial u}{\partial y},\ T = T_w = T_0 + a_1 x,\ C = C_w = C_0 + b_1 x \ \text{ at } \ y = 0$$
$$u \to U_e(x) = ex,\ N \to 0,\ T \to T_\infty = T_0 + a_2 x,\ C \to C_\infty = C_0 + b_2 x \ \text{ when } \ y \to \infty \tag{6}$$

Here u, v indicate liquid velocities (horizontal, vertical), ν – the kinematic viscosity, ρ – the liquid density, k – the vortex viscosity, g – the gravitational acceleration, N – the micro-rotation velocity, β_1, β_2 – the thermal expansion (linear, non-linear) coefficients, T, T_∞ – the temperatures (fluid, ambient), j – the micro-inertia, C, C_∞ – the concentrations (fluid, ambient), β_3, β_4 – the solutal expansion (linear, non-linear) coefficients, γ^* – the spin gradient viscosity, λ_1, λ_2 – the relaxation time fluxes (thermal, solutal), T_0, C_0 – the reference (temperature, concentration), a_1, a_2, c, b_1, b_2, e – the dimensional constants, Q – the coefficient of heat generation, m_0 – the boundary parameter, D – the mass diffusivity, and c_p – the specific heat. The conductivity $K(T)$ dependent on temperature is given:

$$K(T) = K_\infty \left(1 + \varepsilon \frac{T - T_\infty}{T_w - T_0}\right) \tag{7}$$

where K_∞ signify ambient fluid conductivity and ε small parameter.

Employing [11]:

$$\eta = y\sqrt{\frac{c}{\nu}},\quad u = cxf'(\eta),\quad v = -\sqrt{c\nu}\, f(\eta),\quad N = cx\sqrt{\frac{c}{\nu}}\, g(\eta)$$
$$\theta(\eta) = \frac{T - T_\infty}{T_w - T_0},\quad \phi(\eta) = \frac{C - C_\infty}{C_w - C_0} \tag{8}$$

Equations (2)-(6) yield:

$$(1+K)f''' + ff'' - f'^2 + Kg' + \lambda\left[(1+\delta\theta)\theta + N(1+\delta_1\phi)\phi\right] + A^2 = 0 \tag{9}$$

$$\left(1+\frac{K}{2}\right)g'' + fg' - f'g - K(2g - f'') = 0 \tag{10}$$

$$(1+\varepsilon\theta)\theta'' + \varepsilon\theta'^2 + \Pr S\gamma_1(S_1 f' + f'\theta - f\theta') + \Pr S\theta -$$
$$-\Pr(S_1 f' + f'\theta - f\theta') - \Pr\gamma_1\left(S_1 f'^2 + f'^2\theta - ff'\theta - S_1 ff'' - ff''\theta + f^2\theta''\right) = 0 \tag{11}$$

$$\phi'' - \mathrm{Sc}(S_2 f' + f'\phi - f\phi') - \mathrm{Sc}\gamma_2\left(S_2 f'^2 + f'^2\phi - ff'\phi - S_2 ff'' - ff''\phi + f^2\phi''\right) = 0 \tag{12}$$

$$f(0) = 0,\ f'(0) = 1,\ f'(\infty) \to A$$
$$g(0) = -m_0 f''(0),\ g(\infty) \to 0 \tag{13}$$

$$\theta(0) = 1 - S_1,\ \theta(\infty) \to 0 \tag{14}$$

$$\phi(0) = 1 - S_2,\ \phi(\infty) \to 0 \tag{15}$$

Here $K = k/\mu$ denotes material parameter, $A = e/c$ – the velocities ratio, $\lambda = \mathrm{Gr}_x/\mathrm{Re}_x^2$ – the thermal buoyancy factor, $\mathrm{Gr}_x = g\beta_1(T_w - T_0)x^3/\nu^2$ – the thermal Grashof number, $\mathrm{Re}_x = xU(x)/\nu$ – the Reynolds number, $\delta = \beta_2(T_w - T_0)/\beta_1$ – the non-linear thermal convection parameter, $N = \mathrm{Gr}_x^*/\mathrm{Gr}_x$ – the solutal buoyancy factor, $\mathrm{Gr}_x^* = g\beta_3(C_w - C_0)/\nu^2$ – the solutal Grashof number, $\delta_1 = \beta_4(C_w - C_0)/\beta_3$ – the non-linear solutal convection parameter, $\Pr = \mu c_p/K_\infty$ – the Prandtl number, $S_1 = a_2/a_1$ – the thermal stratified variable, $\delta = Q/c\rho c_p$ – the heat generation variable, $(\gamma_1 = \lambda_1 c, \gamma_2 = \lambda_2 c)$ (thermal relaxation time, solutal relaxation time) factors, $S_2 = b_2/b_1$ – the solutal stratified variable, and Sc= ν/D– the Schmidt number.

The coefficient of skin-friction, C_f, is expressed:

$$C_f = \frac{\tau_w}{\rho U_w^2} \tag{16}$$

where τ_w characterizes surface shear stress provided below:

$$\tau_w = \left[(\mu + K)\frac{\partial u}{\partial y} + KN \right]\Bigg|_{y=0} \tag{17}$$

In non-dimensional variables one has:

$$\mathrm{Re}_x^{1/2} C_f = \left[1 + (1 - m_0)K\right] f''(0) \tag{18}$$

Solution procedure and convergence

Here homotopy algorithm is selected for computation of eqs. (9)-(12) subjected to boundary conditions given in eqs. (13)-(15). We select [15]:

$$f_0(\eta) = A\eta + (1 - A)(1 - \mathrm{e}^{-\eta}), \quad g_0(\eta) = m_0 \exp(-\eta)$$
$$\theta_0(\eta) = \exp(-\eta), \quad \phi_0(\eta) = \exp(-\eta) \tag{19}$$

$$L_f = f''' - f', \quad L_g = g'' - g', \quad L_\theta = \theta'' - \theta, \quad L_\phi = \phi'' - \phi \tag{20}$$

where operators $(L_f, L_g, L_\theta, L_\phi)$ expressed in eq. (20) have subsequent properties:

$$L_f(C_1 + C_2\mathrm{e}^{\eta} + C_3\mathrm{e}^{-\eta}) = 0, \quad L_g(C_4\mathrm{e}^{\eta} + C_5\mathrm{e}^{-\eta}) = 0$$
$$L_\theta(C_6\mathrm{e}^{\eta} + C_7\mathrm{e}^{-\eta}), \quad L_\phi(C_8\mathrm{e}^{\eta} + C_9\mathrm{e}^{-\eta}) = 0 \tag{21}$$

in which C_i (i = 1-9) elucidate arbitrary constants.

The implemented scheme *i. e.* HAM involves auxiliary factors $(\hbar_f, \hbar_g, \hbar_\theta, \hbar_\phi)$. These factors effectively regulate series solutions convergence. Plots are portrayed for 13[th] order in fig. 1. Suitable values for $\hbar_f, \hbar_g, \hbar_\theta$, and $\hbar_\phi$ are $-1.25 \le \hbar_f \le -0.35$, $-1.2 \le \hbar_g \le -0.65$, $-1.35 \le \hbar_\theta \le -0.45$, and $-1.3 \le \hbar_\phi \le -0.4$. Moreover, convergence of solutions is confirmed in tab. 1. Cleraly 25[th] order approximations are sufficient for convergence of eqs. (9)-(12).

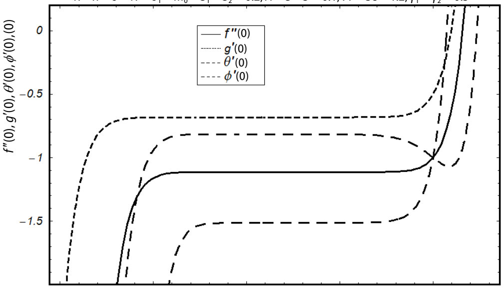

Figure 1. The $\hbar$-curves sketch for f, g, θ, and ϕ

Results

This segment elucidates the extraordinary characteristics of sundry variables *vs.* temperature $\theta(\eta)$, concentration $\phi(\eta)$, and coefficient of skin-friction $\mathrm{Re}_x^{1/2} C_f$ via figs. 2-10.

Influence of ε against $\theta(\eta)$ is scrutinized through fig. 2. As expected $\theta(\eta)$ boosts subject to higher ε estimations. From physical perspective, liquid conductivity augments when ε is increased. As a result, extra heat is transported towards liq-

Table 1. Convergence analysis of governing ordinary expressions for distinct order approximations when $K = \lambda = \delta = N = \delta_1 = m_0 = S_1 = S_2 = 0.2$, $A = \varepsilon = S = 0.1$, $\Pr = \mathrm{Sc} = 1.2$ and $\gamma_1 = \gamma_2 = 0.5$

Order of approximations	$-f''(0)$	$-g'(0)$	$-\theta'(0)$	$-\phi'(0)$
1	1.1375	0.89375	0.9113	1.5875
5	1.1131	0.8851	0.8161	1.5176
10	1.1129	0.8853	0.8147	1.5139
20	1.1129	0.8853	0.8147	1.5139
25	1.1129	0.8853	0.8147	1.5139
30	1.1129	0.8853	0.8147	1.5139

uid from surface and so $\theta(\eta)$ increases. Outcomes of Prandtl number *vs.* $\theta(\eta)$ are expressed through fig. 3. Larger Prandtl number estimation corresponds to less diffusivity which diminishes $\theta(\eta)$ and allied thermal layer. Figure 4 explains γ_1 features on $\theta(\eta)$. It is witnessed that higher values of γ_1 yields $\theta(\eta)$ diminution. Here we noticed non-conducting behavior when γ_1 is augmented. Furthermore, $\theta(\eta)$ improves only for $\gamma_1 = 0$ however it reduces for $\gamma_1 > 0$. Variations of $\theta(\eta)$ subject to S and S_1 are elaborated in figs. 5 and 6. Clearly $\theta(\eta)$ augments for larger S whereas it diminishes subject to larger S_1. Physically, consideration of higher S provides extra heat amount in the system due to which $\theta(\eta)$ rises. Figure 7 reports Schmidt number influence on $\phi(\eta)$. One can see that $\phi(\eta)$ reduces when Schmidt

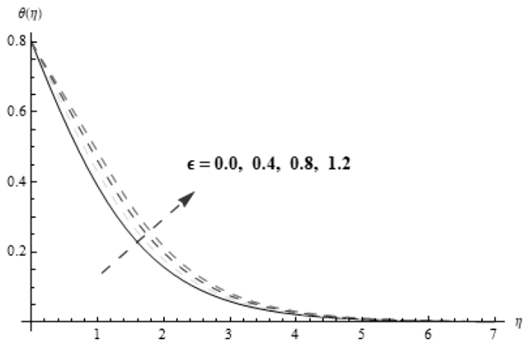

Figure 2. The ε influence *vs.* $\theta(\eta)$

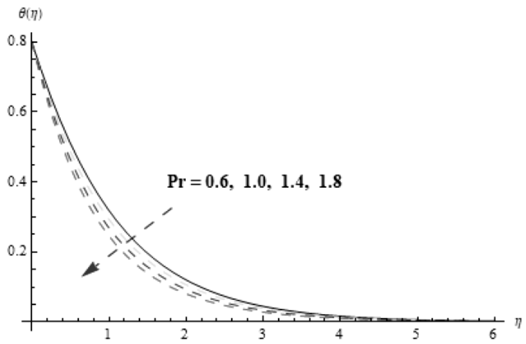

Figure 3. The Pr influence *vs.* $\theta(\eta)$

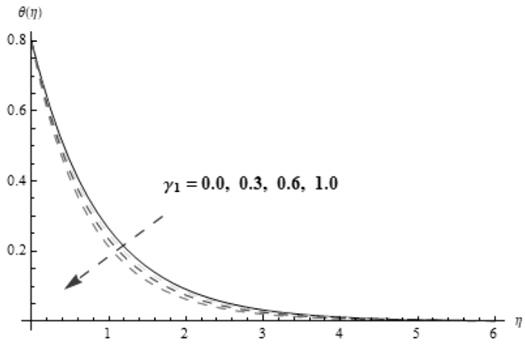

Figure 4. The γ_1 influence *vs.* $\theta(\eta)$

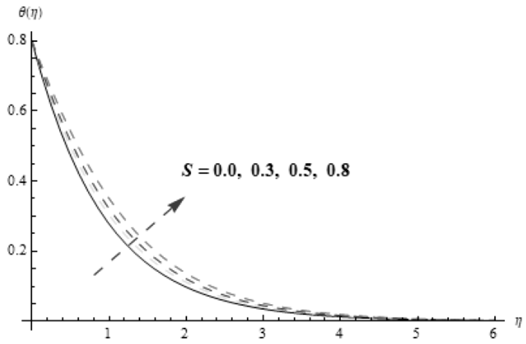

Figure 5. The S influence *vs.* $\theta(\eta)$

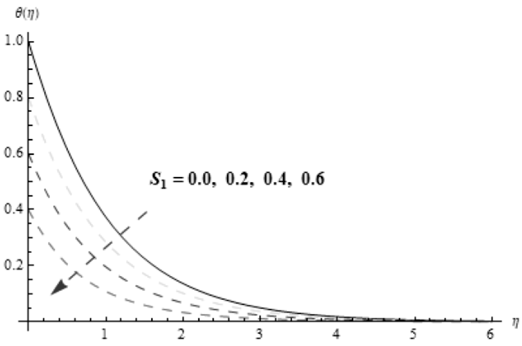

Figure 6. The S_1 influence *vs.* $\theta(\eta)$

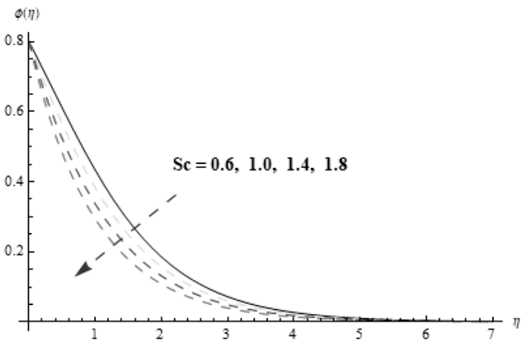

Figure 7. The Sc influence *vs.* $\phi(\eta)$

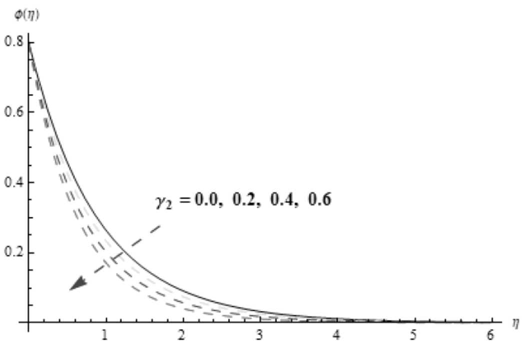

Figure 8. The γ_2 influence *vs.* $\phi(\eta)$

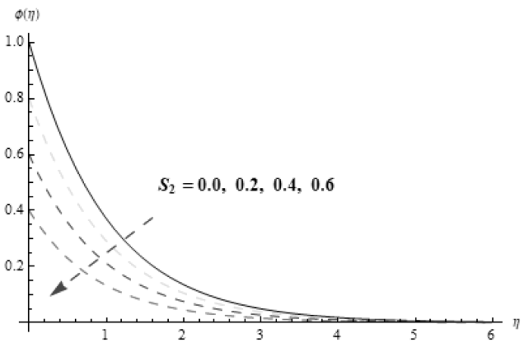

Figure 9. The S_2 influence *vs.* $\phi(\eta)$

number is augmented. In fact the expression of Schmidt number comprises mass diffusivity. In other words, an increase in Schmidt number delivers lowers mass diffusivity. Hence $\phi(\eta)$ decreases. Influences of γ_2 and S_2 against $\phi(\eta)$ are disclosed through figs. 8 and 9. These figsures clearly demonstrate that $\phi(\eta)$ is decreasing function of larger γ_2 and S_2. Figure 10 is portrayed to express the influences of K and m_0 *vs.* $\text{Re}_x^{1/2} C_f$. Here $\text{Re}_x^{1/2} C_f$ rises when K and m_0 are increased.

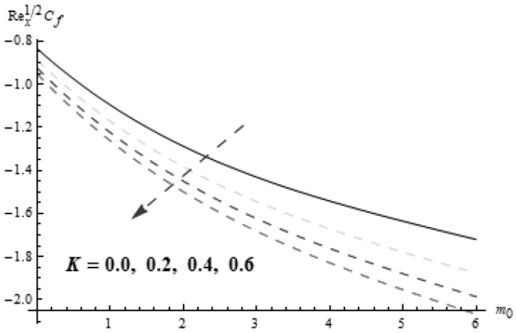

Figure 10. The K and m_0 influences *vs.* $C_f\,\text{Re}_x^{1/2}$

Final remarks

The present investigation has following worth-mentioning points:

- We noticed $\theta(\eta)$ and $\phi(\eta)$ are higher in cases of $\gamma_1 = 0 = \gamma_2$ in comparison to $\gamma_1 > 0$ and $\gamma_2 > 0$.
- Consideration of higher S_1 and ε yield an improvement in $\theta(\eta)$ and $\phi(\eta)$.
- Thermal field $\theta(\eta)$ is lower for both γ_1 and Prandtl number, respectively.
- Heat generation factor, S, causes extra heat amount.
- Coefficient of skin-friction, $\text{Re}_x^{1/2} C_f$, rises when K and m_0 is enhanced.

References

[1] Ozisik, M. N., *Heat Conduction,* (3rd ed.), John Wiley and Sons, New York, USA, 1993
[2] Chen, Z. T., Hu, K. Q., Thermo-Elastic Analysis of a Cracked Half-Plane under a Thermal Shock Impact Using the Hyperbolic Heat Conduction Theory, *Journal of Thermal Stresses, 35* (2012), 4, 342-362
[3] Cattaneo, C., A Form of Heat Conduction Equation which Eliminates the Paradox of Instantaneous Propagation, *Comptes Rendus Mathématique, 247* (1958), pp. 431-433
[4] Vernotee, P., Les Paradoxes de la Theorie Continue de 1 equation del la Chaleur, *Comptes Rendus Mathématique, 246* (1958), pp. 3154-3155
[5] Tzou, D. Y., The Generalized Lagging Response in Small-Scales and High-Rate Heating, *International Journal of Heat and Mass Transfer, 38* (1995), 17, pp. 3231-3240
[6] Christov, C. I., On Frame Indifferent Formulation of the Maxwell-Cattaneo Model of Finite Speed Heat Conduction, *Mechanics Research Communications, 36* (2009), 4, pp. 481-486
[7] Straughan, B., Thermal Convection with the Cattaneo-Christov Model, *International Journal of Heat and Mass Transfer, 53* (2010), 1, pp. 95-98
[8] Haddad, S. A. M., Thermal Instability in Brinkman Porous Media with Cattaneo-Christov Heat Flux, *International Journal of Heat and Mass Transfer, 68* (2014), Jan., pp. 659-668
[9] Liu, L., *et al*., Anomalous Convection Diffusion and Wave Coupling Transport of Cells on Comb Frame with Fractional Cattaneo-Christov Flux, *Communications in Nonlinear Science and Numerical Simulation, 38* (2016), Sept., pp. 45-58
[10] Waqas, M., *et al*., Cattaneo-Christov Heat Flux Model for Flow of Variable Thermal Conductivity Generalized Burgers Fluid, *Journal of Molecular Liquids, 220* (2016), Aug., pp. 642-648
[11] Waqas, M., *et al*., A Generalized Fourier and Fick's Perspective for Stretching Flow of Burgers Fluid with Temperature-Dependent Thermal Conductivity, *Thermal Science,* On-line first, https://doi.org/10.2298/TSCI171025082W
[12] Khan, M. I., *et al*., A Comprehensive Note on Thermally Stratified Flow and Non-Fourier Heat Flux Theory, *Thermal Science,* (2018), doi: 10.2298/TSCI171126140K
[13] Eringen, A. C., Theory of Micropolar Fluids, *Journal of Mathematics and Mechanics, 16* (1966), pp. 1-18
[14] Lukaszewicz, G., *Micropolar Fluids: Theory and Application*, Birkhäuser, Boston, Mass., USA, 1999
[15] Waqas, M., *et al*., Magnetohydrodynamic (MHD) Mixed Convection Flow of Micropolar Liquid Due to Nonlinear Stretched Sheet with Convective Condition, *International Journal of Heat and Mass Transfer, 102* (2016), Nov., pp. 766-772
[16] Shehzad, S. A., *et al*., Flow and Heat Transfer over an Unsteady Stretching Sheet in a Micropolar Fluid with Convective Boundary Condition, *Journal of Applied Fluid Mechanics, 9* (2016), 3, pp. 1437-1445
[17] Asghar, Z., *et al*., Rheological Effects of Micropolar Slime on the Gliding Motility of Bacteria with Slip Boundary Condition, *Results in Physics, 9* (2018), June, pp. 682-691
[18] Benes, M., *et al*., Rigorous Derivation of the Asymptotic Model Describing a Nonsteady Micropolar Fluid Flow Through a Thin Pipe, *Computers and Mathematics with Applications, 76* (2018), 9, pp. 2035-2060
[19] Liao, S., On the Homotopy Analysis Method for Nonlinear Problems, *Applied Mathematics and Computations, 147* (2004), 2, pp. 499-513
[20] Hayat, T., Chemically Reactive Flow of Third Grade Fluid by an Exponentially Convected Stretching Sheet, *Journal of Molecular Liquids, 223* (2016), Nov., pp. 853-860
[21] Khan, W. A., An Improved Heat Conduction and Mass Diffusion Models for Rotating Flow of an Oldroyd-B Fluid, *Results in Physics, 7* (2016), Sept., pp. 3583-3589
[22] Waqas, M., *et al*., Analysis of Forced Convective Modified Burgers Liquid Flow Considering Cattaneo-Christov Double Diffusion, *Results in Physics, 8* (2018), Mar., pp. 908-913
[23] Irfan, M., Modern Development on the Features of Magnetic Field and Heat Sink/Source in Maxwell Nanofluid Subject to Convective Heat Transport, *Physics Letters A, 382* (2018), 30, pp. 1992-2002
[24] Waqas, M., *et al*., Transport of Magnetohydrodynamic Nanomaterial in a Stratified Medium Considering Gyrotactic Microorganisms, *Physica B, 529* (2018), Jan., pp. 33-40
[25] Waqas, M., *et al*., A Theoretical Analysis of SWCNT-MWCNT and H_2O Nanofluids Considering Darcy-Forchheimer Relation, *Applied Nanoscience, 9* (2019), 5, pp. 1183-1191

Paper submitted: October 27, 2017
Paper revised: September 6, 2018
Paper accepted: September 22, 2018